

# Efficiency Improvement of Photoelectrochemical Solar Cell Applications by Using Ternary Hybrid $MoS_2/g - C_3N_4/Cu_2O$

M. Abdurrahman<sup>1</sup>, F.W Burari<sup>2</sup>, O.W Olasoji<sup>2</sup>

<sup>1</sup>Department of physics, faculty of Natural science, Federal University Dutse,  
Jigawa State, Nigeria

<sup>2</sup> Department of physics, faculty of Natural science, Abubakar Tafawa Balewa University  
Bauchi state, Nigeria

\*Corresponding author; Email: [msabduurahman@yahoo.com](mailto:msabduurahman@yahoo.com)

## Article Info

### Article history:

Received , 17/06/2023

Revised, , 17/12/2023

Accepted , 25/05/2024

### Keywords:

Oxidation

Annealing

Photoelectrochemical

Cuprous Oxide

Transition Metals

## ABSTRACT

In this paper, molybdenum disulfide ( $MoS_2$ ) was hybridized with graphene carbon nitrite ( $g - C_3N_4$ ) and  $Cu_2O$  in consideration to heighten the photoelectrochemical (PEC) action and increase the light absorption range of  $Cu_2O$  thin film. The melamine powder was poured in an empty container and then heated in a furnace to attain the  $g - C_3N_4$  powder. The ternary hetero-epitaxial growth was achieved by growing of  $MoS_2/g - C_3N_4$  on the  $Cu_2O$  hybrid by a partial thermal oxidation process. The characteristics of  $MoS_2/g - C_3N_4/Cu_2O$  hybrid film were investigated through XRD, FT-IR and photoelectronchemistry-related measurements. The PEC performance of the treble amalgam electrode was investigated by means of current-voltage test under illumination. The efficiency calculated from current-voltage test under illumination exhibited that the incidence of graphene carbon nitrite and molybdenum disulphide inside the coating networks, regardless of its low down content, may perhaps stimulate substantial improvement in maximum photoconversion effectiveness from 0.036% to 0.33%. This bettering is deducible to the enrichment of the electron-reassign proficiency au courant the incorporation of  $g - C_3N_4$  and  $MoS_2$ , as corroborate by X-Ray Diffraction Analysis (XRD). The PEC investigation results signify that the photoelectrochemical action of the  $MoS_2/g - C_3N_4/Cu_2O$  ternary hybrid is much higher than that of  $Cu_2O$  substrate. The mechanisms accountable for the enhanced PEC behavior of the  $MoS_2/g - C_3N_4/Cu_2O$  triplex hybrid are deliberated in detail.

## I. Introduction

The Industrial rebellion has brought about a fabulous increase in the authentic terrestrial planet subpopulation, and the ultimatum for active energy is increasing [1]. It is anticipated that about nine (9) billion populaces will exist on the globe by the year 2050, and about thirty (30) TW of free energy will be requisite to sustain this populaces [2, 4]. On the other hand, more than 70% of our free energy needs are currently come across by finite black gold, which will soon be exhausted [3-5]. Therefore, using a green backup energy source has turn out to be a big challenge for populace. As a nearly limitless source of green free energy, solar free energy has received substantial consideration in recent period of time. To this closing stages, photoelectrochemical (PEC) cells are considered to be efficient devices for converting solar free energy into hydrogen compound energy by water disserver [6,7]. Photoelectrodes, typically organized of semiconducting material, play the largest part

important roles in luminosity absorption, electron-hole pairing and charge transport in PEC cells [8,9]. However, due to their large bandgaps, most semiconducting materials be able to only engrossed a small portion of daylight in the UV range, which severely limits their potential applications [10].

In order to improve the PEC effectiveness of photoelectrodes, doping by means of compounds or elements and fabrication of semiconductors with heterostructures has been painstakingly on account to the different interactions between different semiconducting materials [11-12]. The progressive or modern candidate of photocathode cuprous oxide ( $\text{Cu}_2\text{O}$ ) has been well thought-out as one them, [13,14].  $\text{Cu}_2\text{O}$  is a usual p-type semiconductor accompanying with a band gap of  $\sim 2$  eV, in the company of which it may possibly accomplish a theoretical photocurrent of  $-14.7 \text{ mAcm}^{-2}$  for water split and a solar to hydrogen translation effectiveness of 18.1 % on the AM 1.5 continuum [14]. Furthermore, it is accessible, globe-copious, ecologically benevolent and companionable with inexpensive fabrication processes that are main necessities requirements to placate the terawatt-scale global free energy demand [15]. The pragmatic applications of  $\text{Cu}_2\text{O}$  in the PEC process is still restricted by two major negative aspect despite the aforementioned advantages: (1) sky-scraping reunification tempo of photogenerated electron-hole carriers, partially endorsed to its inequitable electron diffusion length (usually 20–100 nm) with the light assimilation depth (about 10  $\mu\text{m}$ ) [16]; (2) Deprived photostability by way of self-photocorrosion in electrolyte solution [17]. Configuration engineering has existed stated to efficiently address the above restrictions of  $\text{Cu}_2\text{O}$ . Currently, on account of the plain readiness process, most of  $\text{Cu}_2\text{O}$ -based photocathode for PEC water splitting is built basing on  $\text{Cu}_2\text{O}$  film, frequently displaying a low photoelectric translation effectiveness [18,19]. On the converse, its  $\text{Cu}_2\text{O}$  nanowire/nanorod-based counterparts show appreciably enhanced effectiveness. This is principally attributed to extra proficient light harvesting, more resourceful severance and transport of photogenerated charge carriers, larger exterior area for fast interfacial charge transport, and electrochemical reactions [20- 21]. In addition to structure engineering, heterojunction engineering is widely considered as another effective strategy to improve PEC water splitting performance of  $\text{Cu}_2\text{O}$  through efficient separation of photogenerated charge carriers. [22-23]. The  $\text{Cu}_2\text{O}$ -bound semiconductor is not only a key element in forming the pn junction, but in some cases also acts as a protective layer that slows down the corrosion of the latter [24-25].

Notwithstanding marvelous efforts,  $\text{Cu}_2\text{O}$ -based photocathode contests still remain, and the combination of the above two strategies will lead to the development of a novel and efficient  $\text{Cu}_2\text{O}$ -based photocathode with potential applications in PEC water splitting. It indicates that the continuing need to further explore the photocathode could go further. This work deals with his PEC investigation of his  $\text{Cu}_2\text{O}$  films produced by thermal oxidation. Copper exhibits two dissimilar oxides,  $\text{Cu}_2\text{O}$ , with an unswerving bandgap of 2.1 eV [26,27], so it strongly absorbs barely at wavelengths underneath 600 nm, although  $\text{CuO}$  with a bandgap of 1.21–1.51 eV [28,29] absorbs the entire visible range. In addition, other reasons for choosing  $\text{Cu}_2\text{O}$  as a substance in this analysis are (a) its in large quantity in nature, (b) non-toxicity, (c) low cost of production, and (d) stability and (e) fairly good electrical properties. The effects of ternary hybrid deposition of  $\text{MoS}_2/\text{g} - \text{C}_3\text{N}_4/\text{Cu}_2\text{O}$  film's PEC behavior were investigated. In addition, the films were also characterized in terms of structure and phase analysis using XRD, I-V characteristic curve and FTIR, respectively.

## II. Research Method

### II.1 Synthesis of $\text{Cu}_2\text{O}$ thin film

Commercial pure copper (99.98%) in foil form (0.1 mm thick) was censored into standard size wafers of 2 cm x 2 cm. The sample was pickled on the rim of the bud vase to make it smooth, wrapped up in dilute nitric acid, rinse off thoroughly via distilled water a number of times, and then desiccated to get rid of impurities on the film resurface. After cleaning, the copper film was thermally oxidized by furnace annealing in air. The oxidation temperature was controlled over a wide range beginning from room temperature (RT) to 450 °C. The heating tempo was about 10° C./min, and once the preferred maximum temperature was reached, it was held for 30 minutes to allow copper oxide to form. After oxide formation, the furnace was allowed to cool for 2 hours. Slow cooling was maintained to minimize possible thermal stress and film cracking.

### II.2 Preparation of g-C3N4

In a usual synthesis, the g-  $C_3N_4$  photocatalyst was analyzed disjointedly from melamine [30]. 3.0 g of melamine was naive alumina crucibles with cover and heat up at 500 °C by means of a heating rate of 3 °C min<sup>-1</sup>. It is supplementary heated up to 520 °C for 2 h at a heating rate of 2 °C min and permissible to simmer down to room temperature. A yellow merchandise was gathered and ground into fine particles. The model was named as CN.

### II.3 Synthesis of $MoS_2/g - C_3N_4/Cu_2O$ hybrid film

The technique used to evolve  $MoS_2$  was chemical vapor deposition (CVD) [31, 32]. The substratum was to be set up under specific temperature and pressure conditions and single or a number of precursors were chemically respond on the outer surface of the substratum to fabricate a unsurpassed large-area thin coating. The appliance of CVD in the readying of single-layer TMDs starts with  $MoS_2$  escalation. The heating system tempo was set to 10 °C for each min, the escalation high temperature was 650 °C, and the high temperature was well-kept for 30 min. Once the high temperature was descending to 400 °C, the closure was unlock. The  $MoS_2$  configuration was acquired when the high temperature decreases to room temperature. The investigational procedure was shown in Figure 1.0. CVD can effectively produce monolayer and multilayer  $MoS_2/g - C_3N_4$ . It was able to grow up first-rate single-crystal material and produce thin films consistently distributed over large areas, which were useful in later fabrication of optoelectronic components.



Figure 1. Schematic of a growing  $MoS_2/g - C_3N_4/Cu_2O$  film.

### II.4 Photoelectrochemical tests

For this purpose,  $MoS_2/g - C_3N_4/Cu_2O$  and Cu electrode were arranged and dipped into transparent plastic container. To prepare the electrolyte, the 1g of NaCl powders were mixed with 25 ml of distilled water, stirrer gently until the electrolyte was dissolved completely. The PEC operation of the composite electrodes was evaluated by means of Current-Voltage measurements (Figure 2). The photoelectrochemical experiments were accomplished by means of a two-electrode electrochemical arrangement. A working electrode ( $MoS_2/g - C_3N_4/Cu_2O$ ) and a copper coat were engaged as the counter electrodes, correspondingly. The multimeter was employed to accomplished electrical route of the photo-current density and photo-voltage of electrodes beneath the illumination (AM 1.5 G) within the potential window using 1g of NaCl electrolyte as a mediator between the two electrodes. The draw close described in this study provides a simple and novel method to produce thin coating materials, prepared for practical applications for instance the photoelectrochemical solar cell and hydrogen production.

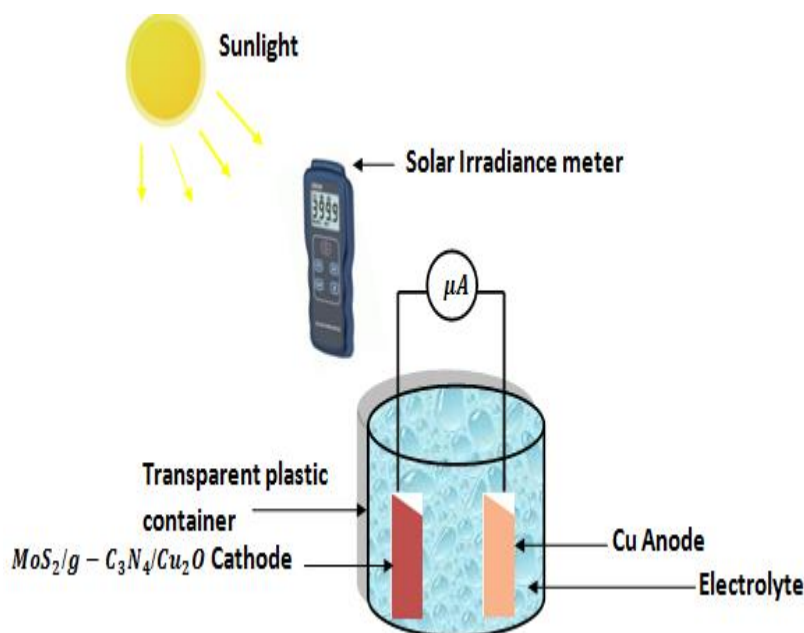


Figure 2: Illustration of the fabricated Cu –  $MoS_2/g - C_3N_4/Cu_2O$  Photoelectrochemical solar cell.

## II.5 Results and Discussion

The crystallized arrangement and the crystallized nature of the thermally oxidized  $MoS_2/g - C_3N_4/Cu_2O$  coatings were examined by XRD investigation. Figure 3 displayed the XRD patterns of  $MoS_2/g - C_3N_4/Cu_2O$  thin films deposited at different thermally oxidized temperature.

XRD patterns show up that the sediment  $Cu_2O$  films are microcrystalline in nature and belong to cubic configuration. In addition, all slightly increasing characteristic peaks from the ternary samples were been examine entirely and their peaks are at  $2\theta$  numerical quantity of  $29.01^\circ$ ,  $36.52^\circ$ ,  $42.11^\circ$  and  $61.11^\circ$  matching to (110), (111), (200) and (220) diffraction plane of  $Cu_2O$  (JCPDS card no. 05-0667), correspondingly, were perceived [33,34,35]. Thermally oxidized  $MoS_2$  the observed peaks at  $33.6^\circ$  correspond to (101) [36].  $37.158^\circ$  displayed peak corresponding to (212) plane of  $g - C_3N_4$ , [37,38,39].  $38.9^\circ$ ,  $43.8^\circ$  and  $52.2^\circ$  corresponding to  $CuO$  (111),  $Cu$  (111) and  $Cu$  (200), [35].  $MoS_2$  also displays peaks that corresponded to (101) at  $33.4^\circ$ , (104) at  $46.1^\circ$  and (008) at  $61.7^\circ$  [40,41]. Table 1 displayed the qualitative analysis result of the triplex sample.

Table 1: Qualitative Analysis Results of the sample

S.No.	Phase name	Formula	Figure of merit
1	Cuprite	$Cu_2O$	0.950
2	Molybdenite-2H	$MoS_2$	2.970
3	Copper	$Cu$	2.448
4	Iron	$Fe$	1.003

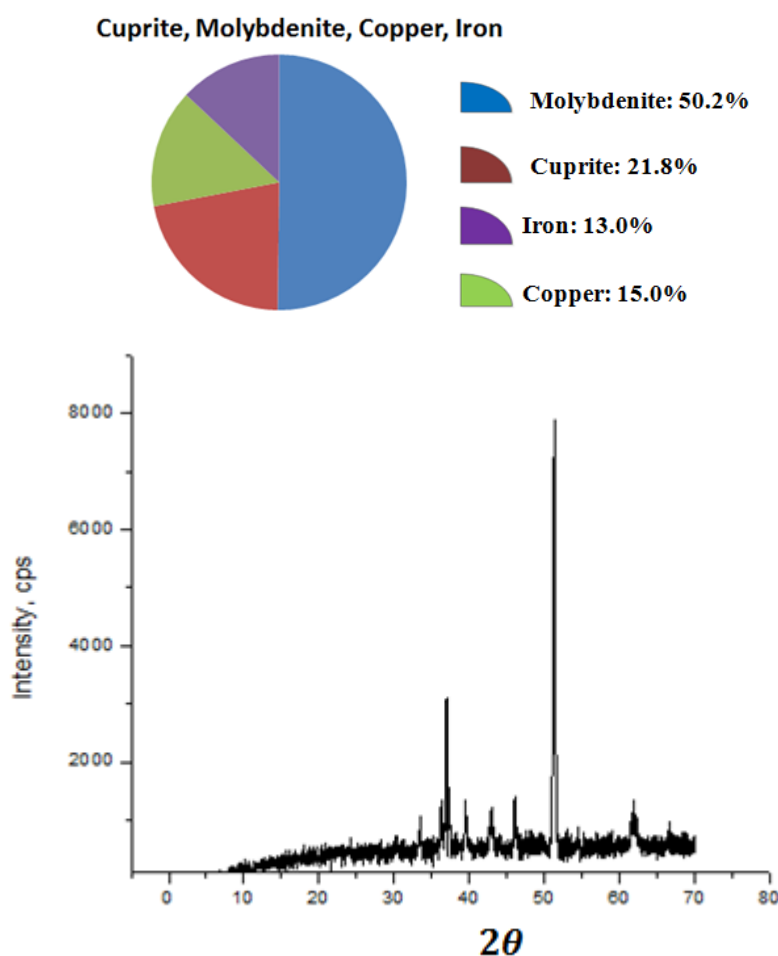


Figure 3. XRD pattern of  $\text{MoS}_2/\text{g-C}_3\text{N}_4/\text{Cu}_2\text{O}$

## II.6 FT-IR spectra analysis

FT-IR investigation (Figure 4.) was performed to analyze the compound and functional properties of mere  $\text{g-C}_3\text{N}_4$ ,  $\text{MoS}_2$ , and  $\text{Cu}_2\text{O}$  thin films. Pure  $\text{g-C}_3\text{N}_4$  exhibits a characteristic IR extremum at  $1632\text{ cm}^{-1}$ , whereas peaks at  $1245$ ,  $1320$  and  $1417\text{ cm}^{-1}$  are imputed to the C-N heterocyclic stretch of  $\text{g-C}_3\text{N}_4$  [42,43]. Broad shoulder bands in the regions of  $3150$ ,  $3320$  and  $3350\text{ cm}^{-1}$  adhered to the elongated modes of the terminal NH groups at the aromatic ring defects [44, 45]. The existence of oxygen-correlated bonds was due to the occurrence of sharp bands regarding  $3620\text{ cm}^{-1}$  [44, 45]. The peak at  $3405\text{ cm}^{-1}$  is ascribed to O-H groups [44, 45], and  $839\text{ cm}^{-1}$  and  $893.39\text{ cm}^{-1}$  are broad absorption bands attributed to  $\text{MoS}_2$  [46, 47]. The peak at  $3506\text{ cm}^{-1}$  is due to the oxygen correlated composite [44, 45]. An extremum of in relation to  $1730\text{ cm}^{-1}$  bespeak the occurrence of C = O bonds in the model. The  $2325\text{-}2425\text{ cm}^{-1}$  band represents the P-H stretch.  $2998\text{-}2959\text{ cm}^{-1}$  is assigned to symmetric C-H stretch vibration. From Figure. 4 it is observed that, the attributed peaks for  $\text{Cu}_2\text{O}$  ( $630\text{ cm}^{-1}$ ) shift (towards lower wavenumber) after the incorporation of  $\text{g-C}_3\text{N}_4$  and  $\text{MoS}_2$ , which bespeak that there was an interface stuck between  $\text{g-C}_3\text{N}_4$ ,  $\text{Cu}_2\text{O}$  and  $\text{MoS}_2$ . From the spectra, all the characteristic peaks of both  $\text{g-C}_3\text{N}_4$ ,  $\text{Cu}_2\text{O}$  and  $\text{MoS}_2$  appeared in the  $\text{MoS}_2/\text{g-C}_3\text{N}_4/\text{Cu}_2\text{O}$ , which is in compliance with the XPS spectrum.

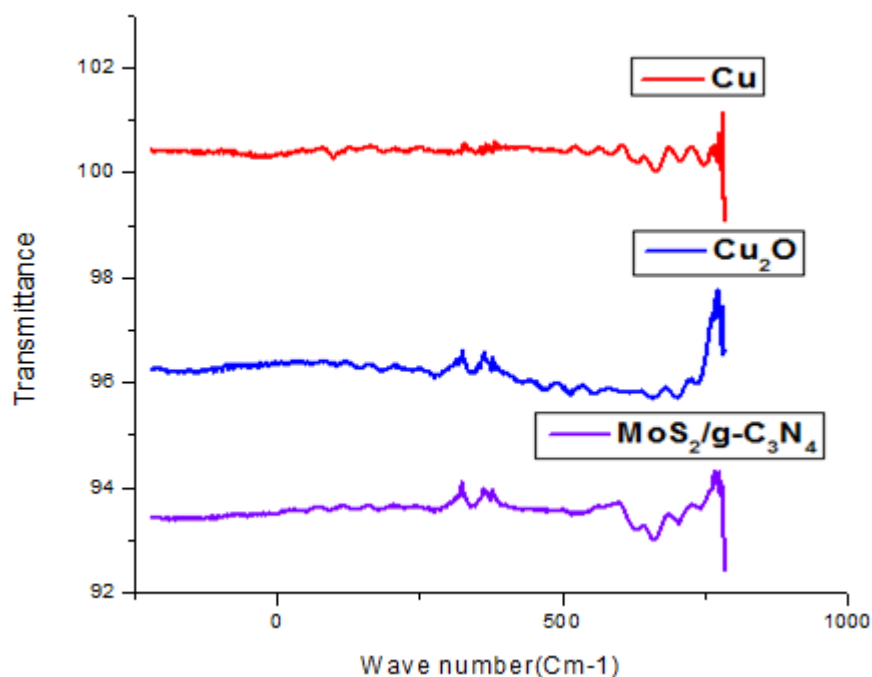


Figure 4. FTIR spectra of  $MoS_2/g - C_3N_4/Cu_2O$

## II.7 I-V Curve analysis

The effectiveness, utmost power, photo voltage and photo-current was acquired neath illumination as lination in Table 2.0 and the Cu- $MoS_2/g - C_3N_4/Cu_2O$  PEC solar cell showed characteristic curves of a number of external parameters followed by transition power efficiency deduce from figure 4 and figure 5. When analyzing the trial product, the deliberate external parametric quantity of the organized samples Cu- $Cu_2O$  and  $MoS_2/g - C_3N_4/Cu_2O$  are avowed as revealed in table 2.0. Two dissimilar readings are recorded by means of a multimeter and frequent solar irradiances in sequence to study the solar cell parameters, two different graphical records are premeditated for two different samples for examining photo response and photo voltage of the electrode under illumination. In table 2.0 it can appear that for the synthesized  $MoS_2/g - C_3N_4/Cu_2O$ , the deposited of 2D materials increases the photo response at the equivalent time escalating the effectiveness of the model. It additional mechanism as an absorber stratum to produces charge carriers (electrons and holes) beneath solar light irradiation. A Comparison of some Findings of  $I_{sc}$ ,  $V_{oc}$  and  $\eta$  with other Works in Literature displayed in table 3 below.

Table 2.0: The photocurrent, utmost power, effectiveness and photo voltage of dissimilar reading of Cu- $Cu_2O$  and Cu- $MoS_2/g - C_3N_4/Cu_2O$  photoelectrochemical solar cell

S/N	Sample	$I_{sc}(mA)$	$V_{oc}(mV)$	$\eta(\%)$
1	$Cu_2O$	0.14	11.0	0.036
2	$MoS_2/g - C_3N_4$	1.20	60	0.33

The foremost row in table 2.0 is for Cu- $Cu_2O$  synthesized using thermal oxidation method while the subsequent row is for - $MoS_2/g - C_3N_4/Cu_2O$  layer deposited by partially thermal oxidation method.

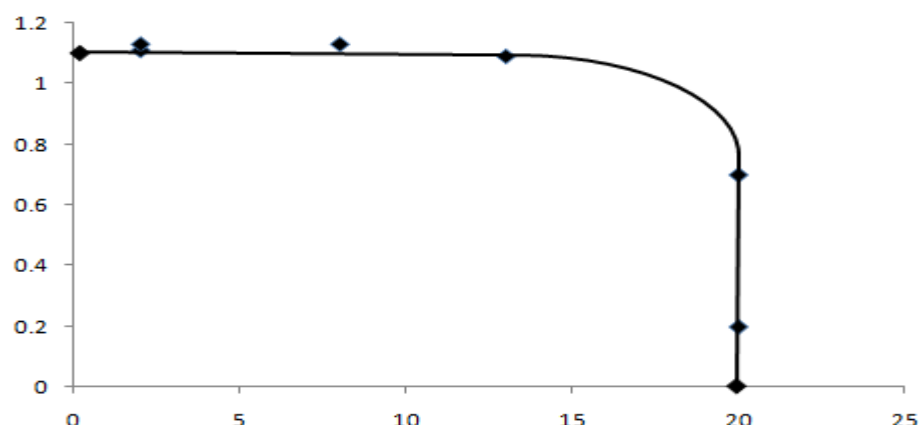


Figure. 4: The graph of Cu-Cu<sub>2</sub>O photoelectrochemical solar cell before surface adjustment

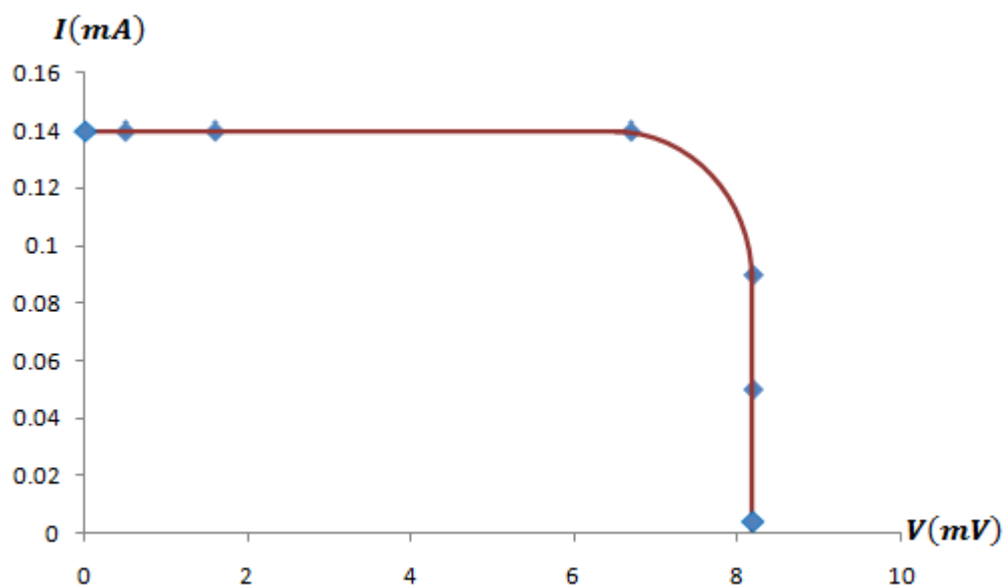


Figure. 5: The graph of Cu- MoS<sub>2</sub>/g - C<sub>3</sub>N<sub>4</sub>/Cu<sub>2</sub>O photoelectrochemical solar cell after surface modification

Table 3: Assessment of Findings with other Works in Literature

Authors (Year)	Structures	Method	Efficiency	findings	References
	Cu <sub>2</sub> O		1%		[48]
J. Herion, et al.,(1979)	Cu/Cu <sub>2</sub> O	partial thermal oxidation	0.4%	V <sub>oc</sub>	
R. P. Wijesundera (2010)	Ti/CuO/Cu <sub>2</sub> O/Au	Electro-deposition	0.02%	FF, Isc, Voc	[49]
Katayama et al (2004)	Cu <sub>2</sub> O/ZnO/ITO	Electro-deposition	0.117%	FF, Isc, Voc	[50]
Septina et al (2011)	Cu <sub>2</sub> O/AZO	Electro-deposition	0.60%	FF, Isc, Voc	[51]
Seyed, A.J (2013)	Cu <sub>2</sub> O	Electro-deposition	0.082%	FF, Isc, Voc	[52]
Y.-K. Hsu, et al (2015)	Cu <sub>2</sub> O	Electro-deposition	0.42	FF, Isc, Voc	[53]
Abdu Y, (2017)	Cu <sub>2</sub> O	Thermal oxidation	0.08	FF, Isc, Voc	[54]
Vijayaraghavan, et al (2018)	CdTe	SPD technique	0.062	FF, Isc, Voc	[55]

Roza, et al (2014)	ZnO	Hydrothermal	0.050	<i>FF, Isc, Voc</i>	[56]
Abdurrahman, M., (2019)	Cu <sub>2</sub> O	Thermal oxidation	0.046	<i>FF, Isc, Voc</i>	[57]
Sutripto, et al (2019)	CdO	chemical method	0.21	<i>FF, Isc, Voc</i>	[58]
Tadatsugu Minami, et al(2016)	Zn <sub>2</sub> GeO <sub>4</sub>	Thin film deposition	0.12	<i>FF, Isc, Voc</i>	[59]
Tadatsugu Minami, et al(2016)	Zn <sub>2</sub> SiO <sub>4</sub>	Thin film deposition	0.03	<i>FF, Isc, Voc</i>	[59]
Tadatsugu Minami, et al(2016)	ZnSnO <sub>3</sub>	Thin film deposition	0.01	<i>FF, Isc, Voc</i>	[59]
This work		Thermal oxidation	0.33	<i>FF, Isc, Voc</i>	
Abdurrahman, M., (2022)	Cu <sub>2</sub> O	Thermal oxidation	4.80	<i>FF, Isc, Voc</i>	[4]

### III. Conclusion

A ternary hybrid composed of  $MoS_2$ ,  $g - C_3N_4$  and  $Cu_2O$  thin film was synthesized for photoelectrochemical solar cell applications. The  $MoS_2/g - C_3N_4$  binary hybrid was prepared by partial thermal oxidation processing of  $MoS_2$  and  $g - C_3N_4$  in a sealed high temperature furnace. The epitaxial growth of  $MoS_2$  and that of  $g - C_3N_4$  on the surfaces of  $Cu_2O$  thin film were taken place during the partial thermal oxidation process. Full structure and PEC analysis specify that the improved PEC activity could be attributed to the synergy between the two 2D materials. In addition, 2D materials exhibit a passivation effect that not only improves photo-excitation voltage and current by tumbling the reunification rate of charge carriers, but also increases surface photoelectrochemical to enhance the photocurrent by rushing the separation of the surface charge and utilization. The subsequent efficacious electric filed stoutness in the space charge coating drastically increases the separation efficiency of photogenerated electron-hole pairs and ultimately enhancing their PEC performances. The synthesized  $MoS_2/g - C_3N_4/Cu_2O$  showed a higher efficiency of 0.33% than that of the  $Cu_2O$  0.036% sample.

### Acknowledgements

I would like to show gratitude TETFUND, Federal University Dutse, for providing favorable environment with free access to laboratory equipment during the research work.

### References

- [1] Asif M., Muneer T. (2007). Energy supply, its demand and security issues for developed and emerging economies, *Renew. Sustain. Energy Rev.* 11, 1388–1411.
- [2] Jacobson M.Z., et al. (2017). 100% clean and renewable wind, water, and sunlight allsector energy roadmaps for 139 countries of the world, *Joule.* 1, 108–121.
- [3] Panwar N.L., Kaushik S.C., Kothari S. (2011). Role of renewable energy sources in environmental protection: a review, *Renew. Sustain. Energy Rev.* 15, 1513–1524.
- [4] Abdurrahman M., Burari F.W., and Olasoji O.W. (2022). Photo electrochemically Manufactured HgO/Cu<sub>2</sub>O Monolayer with Augmented Photovoltaic Features. *Computational and Experimental Research*

- in Materials and Renewable Energy (CERiMRE) Volume 5, Issue 2, page 142-151 eISSN : 2747-173X. doi : 10.19184/cerimre.v5i2.31858
- [5] Mishra A., Mehta A., Basu S., Shetti N.P., Reddy K.R., Aminabhavi T.M. (2019). Graphitic carbon nitride (g-C<sub>3</sub>N<sub>4</sub>)-based metal-free photocatalysts for water splitting: a review, Carbon.
- [6] Hisatomi T., Kubota J., Domen K. (2014) Recent advances in semiconductors for photocatalytic and photoelectrochemical water splitting, Chem. Soc. Rev. 43, 7520–7535.
- [7] Tachibana Y., Vayssieres L., Durrant J.R. (2012). Artificial photosynthesis for solar watersplitting, Nat. Photon. 6, 511
- [8] M. Abdurrahman, F. W Burari, O. W Olasoji, (2023). Facile Fabrication Of Mos<sub>2</sub>/zno Hetero-epitaxial Growth On Cu<sub>2</sub>O With Enhanced Photoelectrochemical Activity Through Thermal Oxidation Process Algerian Journal of Renewable Energy and Sustainable Development, Volume 5, Numéro 2, Pages 118-128
- [9] Grätzel M. (2001). Photoelectrochemical cells, Nature 414, 338.
- [10] Hara K., Horiguchi T., Kinoshita T., Sayama K., Sugihara H., Arakawa H. (2000). Highly efficient photon-to-electron conversion with mercurochrome-sensitized nanoporous oxide semiconductor solar cells, Solar Energy Mater. Solar Cells 64, 115–134.
- [11] Basavarajappa P.S., Bhojya N.H., Seethya N.G., Eshwaraswamy K.B., Kakarla R.R. (2018). Enhanced photocatalytic activity and biosensing of gadolinium substituted BiFeO<sub>3</sub> nanoparticles, Chemistry Select 3 (31), 9025–9033.
- [12] Venkata R.C., Neelakanta Reddy I., Akkinapally B., Reddy K.R., Shim J. (2020). Synthesis and photoelectrochemical water oxidation of (Y,Cu) codoped  $\alpha$ -Fe<sub>2</sub>O<sub>3</sub> nanostructure photoanode, J. Alloys Comp. 814, 152349.
- [13] Akansha Mehta, Amit Mishra, Soumen Basu, Nagaraj P. Shetti, Kakarla Raghava Reddy, Tawfik A. Saleh, Tejraj M. Aminabhavi. (2019). Band gap tuning and surface modification of carbon dots for sustainable environmental remediation and photocatalytic hydrogen production—a review, J. Environ. Manage. 250, 109486.
- [14] Roger I., Shipman M.A., Symes M.D. (2017). Earth-abundant catalysts for electrochemical and photoelectrochemical water splitting, Nature reviews chemistry, 1, 1-13
- [15] Huang Q., Ye Z., Xiao X. (2015). Recent progress in photocathodes for hydrogen evolution, J. Mater. Chem. A 3, 15824-15837.
- [16] Yang Y., Xu D., Wu Q., Diao P. (2016). Cu<sub>2</sub>O/CuO Bilayered composite as a high-efficiency photocathode for photoelectrochemical hydrogen evolution reaction, Sci. Rep. 6, 35158.
- [17] Zhang Z., Dua R., Zhang L., Zhu H., Zhang H., Wang P. (2013). Carbon-layer-protected cuprous oxide nanowire arrays for efficient water reduction, ACS Nano. 7, 1709-1717.
- [18] Mavrokefalos C.K., Hasan M., Rohan J.F., Compton R.G., Foord J.S. (2017). Electrochemically deposited Cu<sub>2</sub>O cubic particles on boron doped diamond substrate as efficient photocathode for solar hydrogen generation, Appl. Surf. Sci. 408, 125-134.
- [19] Bicer Y., Chehade G., Dincer I. (2017). Experimental investigation of various copper oxide electrodeposition conditions on photoelectrochemical hydrogen production, Int. J. Hydrogen. Energ. 42, 6490-6501.
- [20] Shyamal S., Hajra P., Mandal H., Bera A., Sariket D., Satpati A.K., Kundu S., Bhattacharya C. (2016). Benign role of Bi on an electrodeposited Cu<sub>2</sub>O semiconductor towards photo-assisted H<sub>2</sub> generation from water, J. Mater. Chem. A 4, 9244-9252.
- [21] Luo J., Steier L., Son M., Schreier M., Mayer M.T., Graetzel M. (2016). Cu<sub>2</sub>O Nanowire photocathodes for efficient and durable solar water splitting, Nano Lett. 16, 1848-1857.
- [22] Li, X., Yu, J., Jaroniec. M. (2016). Hierarchical photocatalysts, Chem. Soc. Rev. 45, 2603-2636.
- [23] Liu, Y., Ren, F., Shen, S., Fu, Y. Chen, C., Liu, C., Xing, Z., Liu, D. et al., (2015). Efficient enhancement of hydrogen production by Ag/Cu<sub>2</sub>O/ZnO tandem triple-junction photoelectrochemical cell, Appl. Phys. Lett. 106, 123901.
- [24] Cui, W., An, W., Liu, L., Hu, J., Liang, Y. (2014). Novel Cu<sub>2</sub>O quantum dots coupled flower-like BiOBr for enhanced photocatalytic degradation of organic contaminant, J. Hazard. Mater. 280, 417-27.

- [25] Xu, X., Liu, Y., Zhu, Y., Fan, X., Li, Y., Zhang, F., Zhang, G., Peng, W. (2017). Fabrication of a Cu<sub>2</sub>O/g-C<sub>3</sub>N<sub>4</sub>/WS<sub>2</sub> Triplelayer photocathode for photoelectrochemical hydrogen evolution, *Chemelectrochem.* 4, 1498-1502
- [26] Zhang, P., Wang, T., Zeng, H. (2017). Design of Cu-Cu<sub>2</sub>O/g-C<sub>3</sub>N<sub>4</sub> nanocomponent photocatalysts for hydrogen evolution under visible light irradiation using water-soluble Erythrosin B dye sensitization, *Appl. Surf. Sci.* 391, 404-414.
- [27] Golden TD, Shumsky MG, Zhou Y, Nander Werf RA, Van Leeuwen RA, Switzer JA. *ChemMater* (1996);8:2499.
- [28] Nair MTS, Guerrero L, Arenas OL, Nair PK. *Appl Surf Sci* (1990);150:143.
- [29] Marabelli F, Parravicini GB, Drioli FS. *Phys Rev B* (1995);52:1433.
- [30] Ghijsen J, Tjeng LH, Elp JV, Eskes H, Westerink J, Sawatzky GA, Czyzyk MT. *Phy Rev B* (1988);38:11322.[30] Yan SC, Li ZS, Zou ZG. (2010). Photodegradation of rhodamine B and methyl orange over boron-doped g-C<sub>3</sub>N<sub>4</sub> under visible light irradiation. *Langmuir*;26:3894e901.
- [31] Wang, Q.; Lei, Y.; Wang, Y.; Liu, Y.; Song, C.; Zeng, J.; Song, Y.; Duan, X.; Wang, D.; Li, Y. (2020). Atomic-scale engineering of chemicalvapor-deposition-grown 2D transition metal dichalcogenides for electrocatalysis. *Energy Environ. Sci.*, 13, 1593–1616, <https://doi.org/10.1039/d0ee00450b>.
- [32] Najmaei, S.; Liu, Z.; Zhou, W.; Zou, X.; Shi, G.; Lei, S.; Yakobson, B.I.; Idrobo, J.C.; Ajayan, P.M.; Lou, J. (2013). Vapour phase growth and grain boundary structure of molybdenum disulphide atomic layers. *Nat. Mater.*, 12, 754–759, <https://doi.org/10.1038/nmat3673>.
- [33] B.M. Almeida, M.A. Melo Jr, J. Bettini, J.E. Benedetti, A.F. Nogueira, (2015). A novel nanocomposite based on TiO<sub>2</sub>/Cu<sub>2</sub>O/reduced graphene oxide with enhanced solar-light-driven photocatalytic activity, *Appl. Surf. Sci.* 324, 419–431.
- [34] Ganesan, K. P., Anandhan, N., Marimuthu, T., Panneerselvam. R., Amali Roselin A. (2018). Effect of Deposition Potential on Synthesis, Structural, Morphological and Photoconductivity Response of Cu<sub>2</sub>O Thin Films by Electrodeposition Technique. *Acta Metallurgica Sinica (English Letters)* <https://doi.org/10.1007/s40195-019-00876-5>
- [35] Quan-Bao Ma n, Jan P. Hofmann, Anton Litke, Emiel J.M. Hensen , (2015) Cu<sub>2</sub>O photoelectrodes for solar water splitting: Tuning photoelectrochemical performance by controlled faceting. *Solar Energy Materials & Solar Cells* 141 (2015) 178–186. <http://dx.doi.org/10.1016/j.solmat.2015.05.025>
- [36] Quilty, C.D., Housel, L.M., Bock, D.C., Dunkin, M.R., Wang, L., Lutz, D.M., Abraham, A., Bruck, A.M., Takeuchi, E.S., Takeuchi, K.J., Marschilok, A.C. (2019). Ex Situ and Operando XRD and XAS Analysis of MoS<sub>2</sub>: A Lithiation Study of Bulk and Nanosheet Materials, *ACS Applied Energy Materials*, 2, 7635-7646, 10.1021/acsaem.9b01538.
- [37] Ganesh Reddy Surikanti, Pooja Bajaj, and Manorama V. Sunkara. (2019) g-C<sub>3</sub>N<sub>4</sub>-Mediated Synthesis of Cu<sub>2</sub>O To Obtain Porous Composites with Improved Visible Light Photocatalytic Degradation of Organic Dyes, *ACS Omega* XXXX, XXX, XXX-XXX <http://pubs.acs.org/journal/acsofd>
- [38] Wang XC, Maeda K, Thomas A, Takanabe K, Xin G, Carlsson JM, et al. (2009) A metal-free polymeric photocatalyst for hydrogen production from water under visible light. *Nat Mater*;8:76e80.
- [39] Wang Y, Wang XC, Antonietti M. (2012). Polymeric graphitic carbon nitride as a heterogeneous organocatalyst: from photochemistry to multipurpose catalysis to sustainable chemistry. *Angew Chem Int Ed*;51:68e89.
- [40] Visic, B.; Dominko, R.; Gunde, M.K.; Hauptman, N.; Skapin, S.D.; Remskar, M. (2011). Optical Properties of Exfoliated MoS<sub>2</sub> Coaxial Nanotubes-Analogues of Graphene. *Nanoscale Res. Lett.*, 6, 593
- [41] Paloma Martínez-Merino , Rodrigo Alcantara , Pedro Gomez-Larran , Ivan Carrillo Berdugo , Javier Navas , (2022). MoS<sub>2</sub>-based nanofluids as heat transfer fluid in parabolic trough collector technology, *Renewable Energy* 188, 721e730, <https://doi.org/10.1016/j.renene.2022.02.069>
- [42] Wang Y, Shi R, Lin J, Zhu Y. (). Enhancement of photocurrent and photocatalytic activity of ZnO hybridized with graphitelike-C<sub>3</sub>N<sub>4</sub>. *Energy Environ Sci* 2011;4:2922e9.
- [43] Chai, B., Peng, T., Mao J, Li, K., Zan, L. (2012). Graphitic carbon nitride (g-C<sub>3</sub>N<sub>4</sub>)ePt-TiO<sub>2</sub> nanocomposite as an efficient photocatalyst for hydrogen production under visible light irradiation. *Phys Chem Chem Phys*;14:16745e52.

- [44] Nandiyanto, A. B. D., Andika, R., Aziz, M., and Riza, L. S. (2019). How to Read and Interpret FTIR Spectroscopy of Organic Material. *Indonesian Journal of Science and Technology*, 3(2), 82-94.
- [45] Nandiyanto, A. B. D., Andika, R., Aziz, M., and Riza, L. S. (2018). Working Volume and Milling Time on the Product Size/Morphology, Product Yield, and Electricity Consumption in the Ball-Milling Process of Organic Material. *Indonesian Journal of Science and Technology*, 3(2), 82-94.
- [46] Zhang, Y.; Chen, P.; Wen, F.; Huang, C.; Wang, H. (2016). Construction of polyaniline/ molybdenum sulfide nanocomposite: Characterization and its electrocatalytic performance on nitrite. *Ionics*, 22, 1095–1102.
- [47] Jaleel, U.C.; Devi, K.R.; Madhushree, P. (2021). Statistical and Experimental Studies of MoS<sub>2</sub>/g-C<sub>3</sub>N<sub>4</sub>/TiO<sub>2</sub>: A Ternary Z-Scheme Hybrid Composite. *J. Mater. Sci.*, 56, 6922–6944.
- [48] J. Herion, *et al.*, (1979). "preparation and analysis of cu<sub>2</sub>o thin-film solar cells.," *Journal of Applied Metalworking*, pp. 917-924, 1979.
- [49] R. P. Wijesundera. (2010). "Fabrication of the CuO/Cu<sub>2</sub>O heterojunction using an electrodeposition technique for solar cell applications," *Semiconductor Science and Technology*, vol. 25, p. 045015, 2010.
- [50] J. Katayama, *et al.*, (2004). "Performance of Cu<sub>2</sub>O/ZnO Solar Cell Prepared By Two-Step Electrodeposition," *Journal of Applied Electrochemistry*, vol. 34, pp. 687-692, 2004/07/01.
- [51] Septina, W. *et al.*, (2011). "Potentiostatic electrodeposition of cuprous oxide thin films for photovoltaic applications," *Electrochimica Acta*, vol. 56, pp. 4882-4888.
- [52] Seyed, A.J., (2013). Electro Deposition of Cuprous Oxide for Thin Film Solar Cell Applications, pp. 04–39
- [53] Hsu, Y.-K. *et al.* (2015). Fabrication Of homojunction Cu<sub>2</sub>O Solar cells by electrochemical deposition, *Appl.Surf.Sci.*, <http://dx.doi.org/10.1016/j.apsusc.2015.05.142>
- [54] Abdu Y. (2017). Fabrication and study of the electrical properties of copper (cu) – cuprous oxide (Cu<sub>2</sub>O) photoelectrochemical solar cell. *Bayero Journal of Sciences* Vol. 8 No. 1, September, 2017, pp 180 – 186
- [55] Vijayaraghavan, S. N., Aditya Ashok, Gopika Gopakumar, Harigovind Menon, Shantikumar V. Nair , Mariyappan Shanmugam .(2018). All spray pyrolysis-coated CdTe TiO<sub>2</sub> heterogeneous films for photo-electrochemical solar cells. *Materials for Renewable and Sustainable Energy* 7:12. [doi.org/10.1007/s40243-018-0120-1](https://doi.org/10.1007/s40243-018-0120-1)
- [56] Roza, L., Rahman, M.Y.A., Umar, A.A., Salleh, M.M. (2014). Direct growth of oriented ZnO nanotubes by self-selective etching at lower temperature for photo-electrochemical (PEC) solar cell application, *Journal of Alloys and Compounds*, doi: <http://dx.doi.org/10.1016/j.jallcom.2014.08.113>
- [57] Abdurrahman, M. (2019). Manufacture and study of the electrical properties of copper (cu) – cuprous oxide (Cu<sub>2</sub>O) photoelectrochemical solar cell. *FUDMA Journal of Sciences (FJS)* Vol. 3 No. 2, June, 2019, pp 167 – 172
- [58] Sutripto Majumder, Avinash C. Mendhe, Dojin Kim, Babasaheb R. Sankapal (2019). CdO nanonecklace: Effect of air annealing on performance of photo electrochemical cell. [doi.org/10.1016/j.jallcom.2019.02.159](https://doi.org/10.1016/j.jallcom.2019.02.159)
- [59] Tadatsugu Minami., Yuki Nishi., and Toshihiro Miyata. (2016). Cu<sub>2</sub>O-based solar cells using oxide semiconductors. Vol. 37, No. 1. *Journal of Semiconductors*. Doi: 10.1088/1674-4926/37/1/014002